Design Guideline for PWM Converter Implementing Periodic VSFPWM
A Comprehensive Analysis on the Harmonics Spectrum

Wu, Yang; Qin, Zian; Soeiro, Thiago B.; Bauer, Pavol

DOI
10.23919/ICPE2023-ECCEAsia54778.2023.10213757

Publication date
2023

Document Version
Final published version

Published in
Proceedings of the 2023 11th International Conference on Power Electronics and ECCE Asia (ICPE 2023 - ECCE Asia)

Design Guideline for PWM Converter Implementing Periodic VSFPWM —A Comprehensive Analysis on the Harmonics Spectrum

Yang Wu[1], Zian Qin[1], Thiago Bastia Soeiro[2] and Pavol Bauer[1]
[1] DCE&S Group, Delft University of Technology, The Netherlands
[2] PE Group, University of Twente, The Netherlands
Email: Y.Wu-6@tudelft.nl; Z.Qin-2@tudelft.nl; t.batistasoeiro@utwente.nl; P.Bauer@tudelft.nl

***Abstract*—With the great emphasis from the international standard-setting community on the so-called supra-harmonics emissions (2-150 kHz), there are increasing research efforts in this noise level identification, measurement, standard setting and mitigation. The periodic variable switching frequency PWM method, which is known as VSFPWM, can reshape the generated output harmonics spectrum of the grid-connected PWM converter, leading to a significantly lower harmonics peaks, thus keeping the harmonics emission strictly below the harmonics emission standards e.g., IEEE519 & IEC-61000 series. This work conducted an insightful analysis on the harmonics spectra generated by the periodic VSFPWM based on newly derived analytical models. Besides, the sinusoidal VSFPWM which is often used in AC/DC PWM converter, is taken as an example of periodic VSFPWM profile to achieve the minimum efforts of AC filtering. Finally, experimental tests are conducted to verify the analysis and the design guideline provided in this paper.**

***Index Terms*—Periodic variable switching frequency PWM, supra-harmonics, AC/DC converter, harmonic spectrum.**

I. Introduction

Due to the rapid development of renewable energy integration and E-mobility, the pulse-width-modulation (PWM)-based voltage source converters (VSCs) play a critical role in the associated grid-connection applications because of their robustness and simplicity. In recent years, there are more and more research focus on different modulation techniques to improve the converter efficiency [1], [2] and the ripples of the converter current and DC link voltage [3], [4] for a more compact and efficient power electronics converter system.

Typically the frequency modulation methods adopted in the literatures, for instance the S-TCM method [5] for the zero-voltage switching (ZVS) operation in AC/DC converter and space-vector-modulation based approaches [6], [7] to minimizing the switching loss and output ripples, exhibit a periodicity in the variable switching frequency. Besides, periodic VSFPWM [8], [9] has been proposed to suppress the conducted EMI and reshape the switching harmonics to comply with the supra-harmonics and EMI standards [10]–[12], as depicted in Fig.1. However, none of these works have provided quantitative analysis on the frequency spectrum of the converter output.

This paper provides a general design guideline for the use of periodic variable switching frequency (Periodic-VSFPWM) method based on a comprehensive analysis on the reshaped harmonics spectra of the PWM converter output. The influence of the switching frequency profile has been investigated and analyzed based on the derived analytical models. Both simulation and experiment are conducted to verify the insights drawn from the analysis.

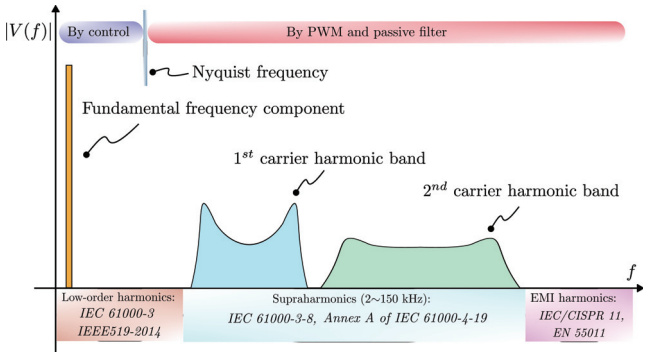

Fig. 1. Overlap of the switching harmonics under the VSFPWM methods.

II. Modeling of P-VSFPWM in 2-Level Converter

In order to provide a general analysis on the harmonic spectrum resulted by the periodic VSFPWM on a three-phase PWM converter, the conventional 2-level-based three-phase PWM converter depicted in Fig.2 is chosen as the studied topology in this work because of its simplicity and modularity. A generic periodic switching frequency $f_{\mathrm{c}}(t)$ can be expressed as the following Fourier series:

$$f_{\mathrm{c}}(t) = f_{\mathrm{c0}} + \sum_{k=1}^{\infty} C_{\mathrm{k}} \cdot \sin(2\pi k f_{\mathrm{m}} t + \theta_{\mathrm{k}}) \tag{1}$$

where f_{c0} is the centered switching frequency and f_{m} is the frequency of the periodic switching frequency profile. According to [9], the switching harmonics of the converter output voltage (voltage between midpoints of DC link and bridges) under SPWM can be hence calculated as follows:

$$v_{\mathrm{c}}(t) = \Re\Big(\sum_{m=0}^{\infty}\sum_{n=-\infty}^{\infty}\sum_{l=-\infty}^{\infty}\{C_{\mathrm{mn}} \cdot h(m,l) \cdot e^{\mathrm{j}(\mathrm{m}\theta_{\mathrm{c}}+\mathrm{n}\theta_{\mathrm{o}}+\varphi_{\mathrm{m}})} \cdot e^{\mathrm{j}2\pi(\mathrm{mf_{c0}t}+\mathrm{nf_{o}t}+\mathrm{lf_{m}t})}\}\Big) \tag{2}$$

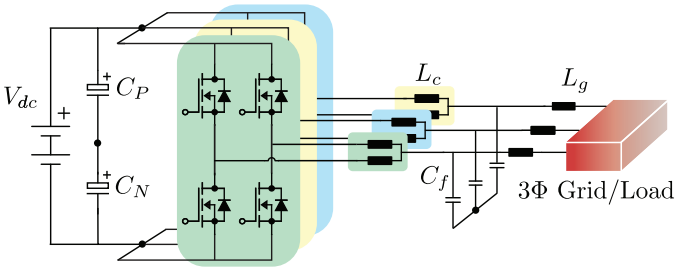

Fig. 2. Three-phase PWM converter circuit working as both 2-hard-paralleling and 2-interleaved 2-level VSC topologies.

$$h(m,l) = \sum_{\sum r_k \cdot k = l} \left(\prod_{k=1}^{\infty} J_{\mathrm{r}}\left(\frac{mC_{\mathrm{k}}}{kf_{\mathrm{m}}}\right) \cdot e^{\mathrm{j(r}(\theta_{\mathrm{k}} - \pi/2))}\right) \quad (3)$$

where m and n are the integer multiples of the carrier and reference signal frequencies. J_{r} is the Bessel function of the first kind and C_{mn} is the magnitude of the harmonics under the constant switching frequency PWM (CSFPWM). Typically for the case of sinusoidal-PWM (SPWM) with symmetrical sampling, C_{mn} becomes:

$$C_{\mathrm{mn}} = \frac{2V_{\mathrm{dc}} J_{\mathrm{n}}[(m + n\frac{\omega_{\mathrm{o}}}{\omega_{\mathrm{c0}}})\frac{\pi M}{2}]}{\pi(m + n\frac{\omega_{\mathrm{o}}}{\omega_{\mathrm{c0}}})} \sin[(m + n\frac{\omega_{\mathrm{o}}}{\omega_{\mathrm{c0}}} + n)\frac{\pi}{2}] \quad (4)$$

where J_{n} is also the Bessel function of the first kind. M is the modulation index given by $M = 2V_{\mathrm{ac}}/V_{\mathrm{dc}}$. The phase φ_{m} shown in (2), which is caused by the P-VSFPWM, can be expressed as:

$$\varphi_{\mathrm{m}} = \sum_{k=1}^{\infty} \varphi_{\mathrm{mk}} = \sum_{k=1}^{\infty} \frac{mC_{\mathrm{k}} \cos(\theta_{\mathrm{k}})}{kf_{\mathrm{m}}} \quad (5)$$

Besides, θ_{c} and θ_{o} are the initial phases of the carrier and reference signals in the PWM process. Typically in a regular PWM with symmetrical sampling, θ_{c} and θ_{o} become 0 when they are implemented as depicted in Fig.3.

III. Symmetry Property of the Harmonic Spectrum

A. Spectrum Symmetry of the Single Spectrum

Based on (2)-(4), the frequency-domain voltage harmonic model implies that a switching harmonic generated by periodic VSFPWM at certain frequency is a combination of infinite individual harmonic terms with their own magnitudes and phases. Besides, the spreading pattern (height and width) of the spectrum is closely related to the parameters of the switching profile: C_{k} and f_{m}, which are selected to be multiples of the fundamental frequency f_{o} for a better compliance with the harmonics standard. For practical use of this model to calculate or predict the spectrum, only limited terms are selected and then calculated since the original harmonic magnitude A_{mn} generated by the CSFPWM are non-zero at only certain frequencies. Under CSFPWM, the left and right sideband harmonics within the carrier harmonic band exhibit a symmetry in the spectrum of the converter output voltage. Under periodic VSFPWM, such a symmetry depends on the

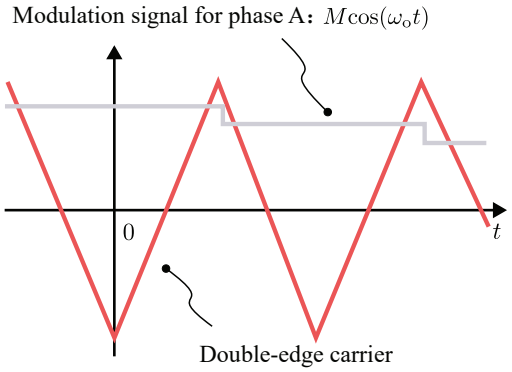

Fig. 3. Reference and carrier signal in a regular PWM process with symmetrical sampling.

frequency of the switching frequency profile f_{m} and the phases θ_{k}. For instance, the converter output voltage, expressed as the sum of the common-mode (CM) and differential-mode (DM) components, and its DM components in the first carrier band are depicted in Fig.4 with the purely sinusoidal switching frequency profile, where k=1, C_{k}=6 kHz, f_{c0} =24 kHz and f_{m} is selected to be different multiples (from 1 to 6) of f_{m}.

It can be noted from Fig.4 that the symmetry of the voltage harmonic spectrum depends on the phase θ_{k}. Several insight can be drawn: (1) The spectrum varies according to θ_{k} values. (2) At $\theta_{\mathrm{k}} = 0°$ or $180°$, the spectral symmetry is still maintained regardless of the ratio between f_{m} and f_{o}. (3) When $f + \mathrm{m}$ is even multiple of f_{o}, the spectrum shows the different levels of asymmetry at other angles.

Apart from θ_{k}, Fig.4 also shows that the simulated harmonics spectrum is symmetrical with f_{m} being even multiples of f_{o} while asymmetric spectrum is presented with odd multiples. Additionally the asymmetry also degrades with the increase of f_{m}: the voltage spectra under the case f_{m}=6f_{o} are in fact asymmetrical though they appear symmetrical from the figure. To be more specific, the maximum difference between the left and right part spectrum is below 2 V. And this difference will decrease further with higher f_{m}. The reliance of the spectral asymmetry on f_{m} can be explained by (4) since the Bessel function has the following property:

$$J_{\mathrm{r}}(\zeta) = (-1)^r J_{-\mathrm{r}}(\zeta) \quad (6)$$

At the side-band $nf_{\mathrm{o}} + rf_{\mathrm{m}}$ and $-nf_{\mathrm{o}} - rf_{\mathrm{m}}$, there are infinite combinations of n and k values as expressed by (7):

$$\begin{aligned} nf_{\mathrm{o}} + rf_{\mathrm{m}} &= n_1 f_{\mathrm{o}} + r_1 f_{\mathrm{m}} \\ &= n_2 f_{\mathrm{o}} + r_2 f_{\mathrm{m}} \\ &= n_3 f_{\mathrm{o}} + r_3 f_{\mathrm{m}} \\ &= \quad \cdots\cdots \\ &= n_i f_{\mathrm{o}} + r_i f_{\mathrm{m}} = N f_{\mathrm{o}} \end{aligned} \quad (7)$$

It is noteworthy that the original harmonic band at n is non-zero and has only choices of even numbers [8]. This indicates a new constraint: $\Delta n f_o = -\Delta r f_m$. When f_{m} is odd multiple of f_{o}, Δr has to be even numbers which consequently ensures

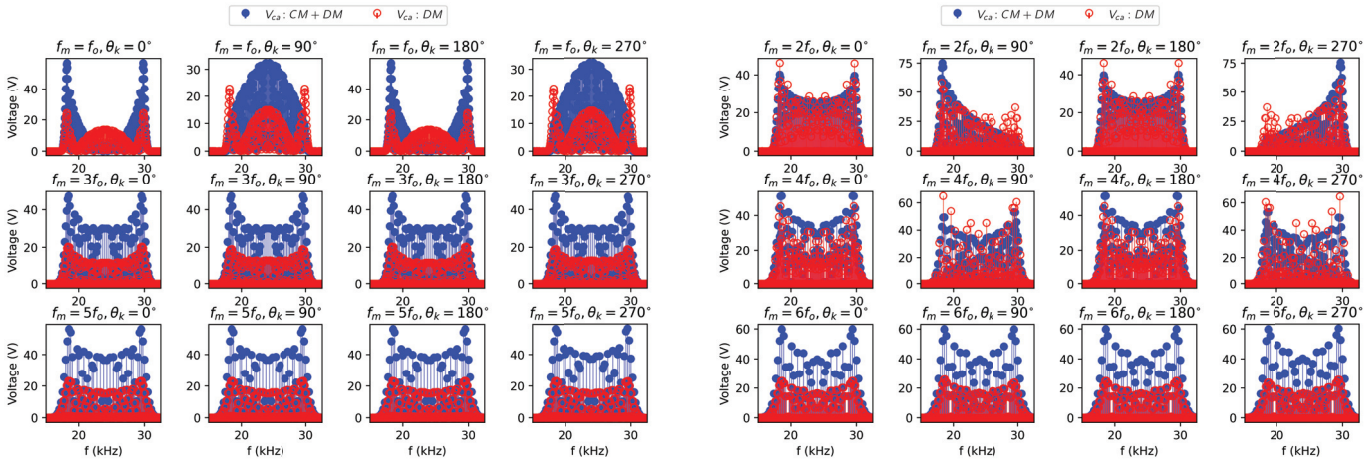

(a) f_{m} is odd multiple of f_{o}

(b) f_{m} is even multiple of f_{o}

Fig. 4. Harmonic spectrum of the converter's output voltage (Phase A) in the first carrier band at different f_{m} and θ_{k}

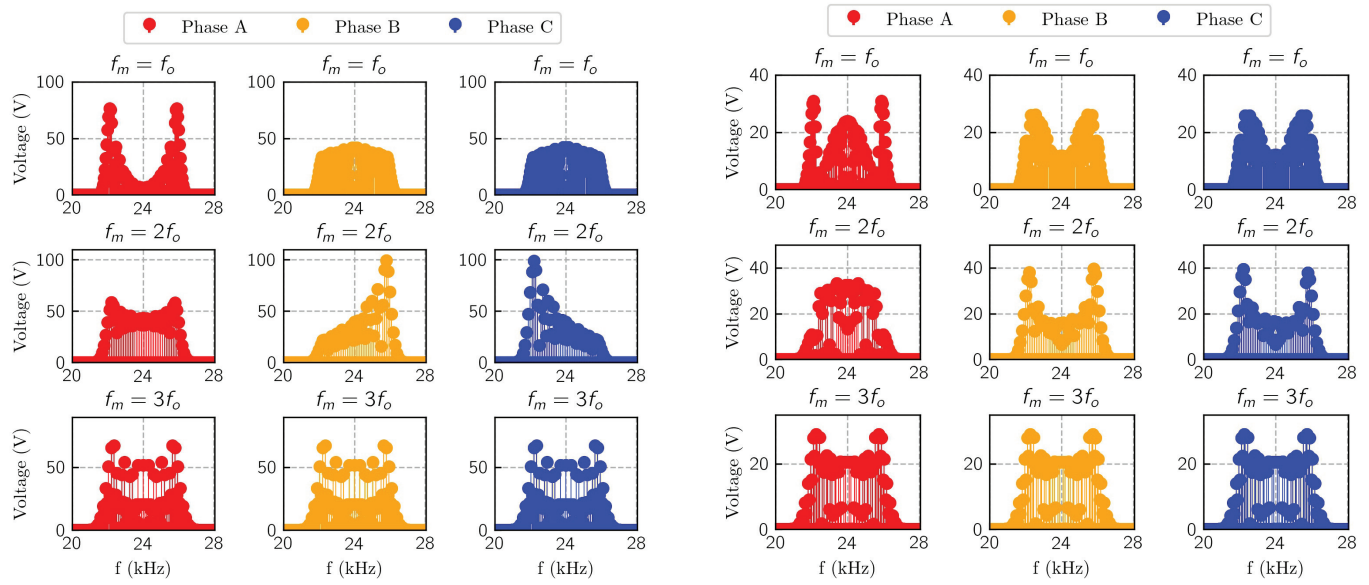

(a) Common-mode + Differential-mode voltage harmonics

(b) Differential-mode voltage harmonics

Fig. 5. Harmonic spectra of the converter's three-phase output voltages in the first carrier band at different f_{m} (same frequency profile for three phases).

an equal harmonic magnitude at the same positive and negative sidebands based on (2)-(6). On the contrary, the spectral symmetry is not guaranteed with f_{m} equal to the even multiple of f_{o}.

B. Spectrum Symmetry between Three Phases

The three phase harmonics are balanced on the condition that the three phase voltages and currents are balanced. However, the harmonic spectra of the three phases might not be symmetrically balanced, indicating a higher harmonic peak in one of the three phases. This will poses extra filtering efforts compared to the three-phase symmetrical spectra. Thus, it is necessary to investigate the symmetry property between the phases. In most scenarios of the periodic VSFPWM implementation in a three-phase PWM converter, the switching frequency profiles between the three phases are the same in shape but differ from each other in terms of phase. Then the three phase converter output voltages (CM+DM components) have the same spectra under such a scenario. However, the DM components, which are mostly concerned in terms of the filter design in three-wire three-phase grid-connected applications, might differ from each other depending on the f_{m}. In the aforementioned situation, the phases of the reference signals under phase a, b and c are:

$$\begin{cases} \theta_{\mathrm{oa}} = \theta_{\mathrm{o}} \\ \theta_{\mathrm{ob}} = \theta_{\mathrm{o}} - \frac{2\pi}{3} \\ \theta_{\mathrm{oc}} = \theta_{\mathrm{o}} + \frac{2\pi}{3} \end{cases} \tag{8}$$

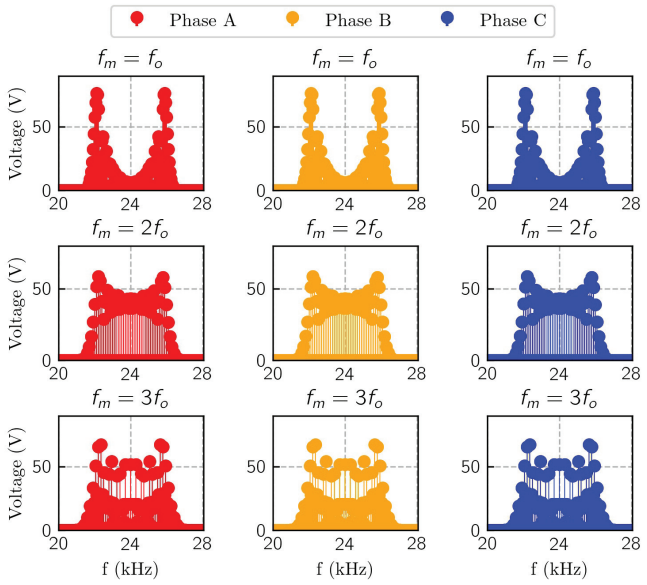

(a) Common-mode + Differential-mode voltage harmonics

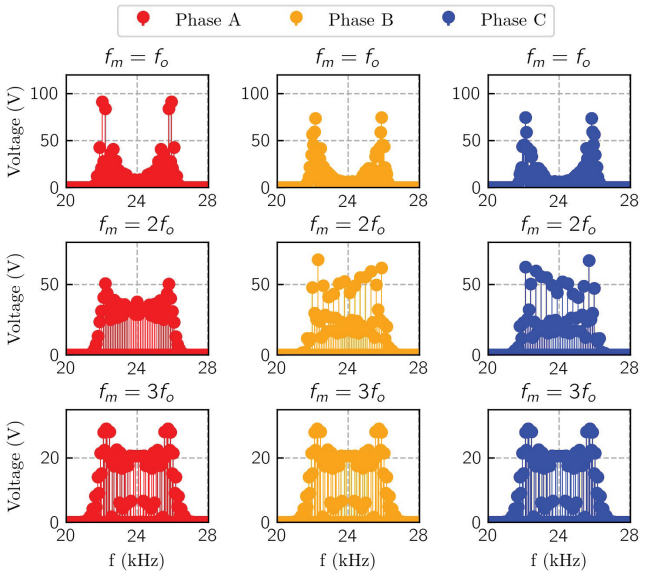

(b) Differential-mode voltage harmonics

Fig. 6. Harmonic spectra of the converter's three-phase output voltages in the first carrier band at different f_{m} (different frequency profiles for three phases).

Similarly, the phases of the carrier signals are:

$$\begin{cases} \theta_{\mathrm{ka}} = \theta_{\mathrm{k}} \\ \theta_{\mathrm{kb}} = \theta_{\mathrm{k}} - \frac{2\pi k f_{\mathrm{m}}}{3 f_{\mathrm{m}}} \\ \theta_{\mathrm{kc}} = \theta_{\mathrm{k}} + \frac{2\pi k f_{\mathrm{m}}}{3 f_{\mathrm{m}}} \end{cases} \tag{9}$$

Based on (2), (4), (8) and (9) it can be noted that the CM harmonic components exist at frequency where n is triple multiple (0,3,6,9…) if f_{m} is triple multiple of f_{o}. Hence the rest harmonics with n equal to non-triples are the DM harmonic components of the three phases voltages, which are identical in terms of the magnitude as observed from the above equations. On the other hand, the CM harmonics components do not necessarily only exist at frequency with n is triple multiple if f_{m} is non-triple multiple of f_{o}. Hence the DM components of the three-phase voltage will not remain the same. This insight is verified by the simulation results presented in Fig.4, where the three phase spectra are identical when $f_{\mathrm{m}} = 3f_{\mathrm{o}}$ and different in other cases. For Fig.5, the frequency profile: $f_{\mathrm{c0}} = 24$ kHz, $C_{\mathrm{k}} = 2$ kHz, $\theta_{\mathrm{k}} = 0°$ is applied to all three phases for simulation validation. In Fig.6, the frequency profile with $f_{\mathrm{c0}} = 24$ kHz, $C_{\mathrm{k}} = 2$ kHz but different θ_{k} expressed by (9) is used for the three phases. In the former case, the results show that both CM+DM and DM harmonics are not magnitude-symmetrical between the three phases except the case of $f_{\mathrm{m}} = 3f_{\mathrm{o}}$. For the latter, the simulation results show that the original spectra (CM+DM) of the three phase converter output voltages are anyway the same in magnitude. However, the magnitude of the DM components become the same between the three phases only when f_{m} is triple multiple of f_{o}.

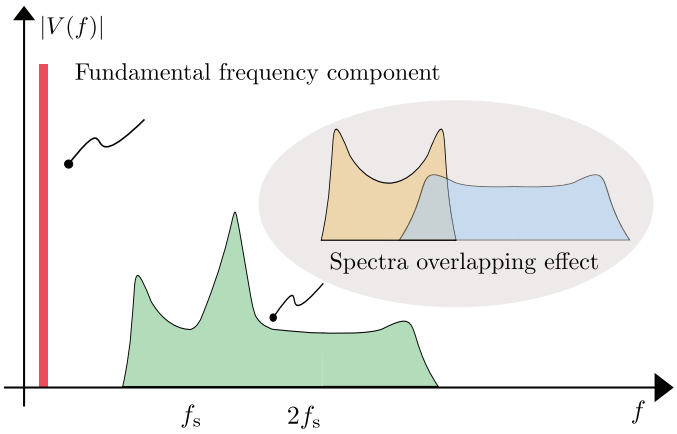

Fig. 7. Overlap between different carrier harmonic bands.

IV. Spectra Overlapping between Carrier Harmonic Bands

In the previous sections, the variation band f_{b} (or C_{k} mentioned in this work) of the switching frequency profile is studied and simulated with quite small values. In real scenarios of the P-VSFPWM implementation, for instance the S-TCM in the 2-level PWM converter, the switching frequency profiles shows a quite larger variation so that the first and second carrier bands overlap and form a much higher harmonic resonance peak, as shown in Fig.7. To avoid or to cancel out this overlapping phenomenon, the interleaved topology is suggested in this paper. Only the even carrier harmonic bands exist in the spectra if the number of interleaving bridges of the converter is two. Fig.6 shows the grid currents and their spectra of the 6.6kW three-phase two-level (non-interleaving,

TABLE I
SYSTEM PARAMETERS.

P_{rated} [kW]	V_{dc} [V]	$V_{\text{g-rms}}$ [V]	ω_{o} [rad/s]	L_{c} [μ H]	L_{g} [μ H]	C_{f} [μF]
6.6	700	230	$2\pi{\cdot}50$	360	720	5

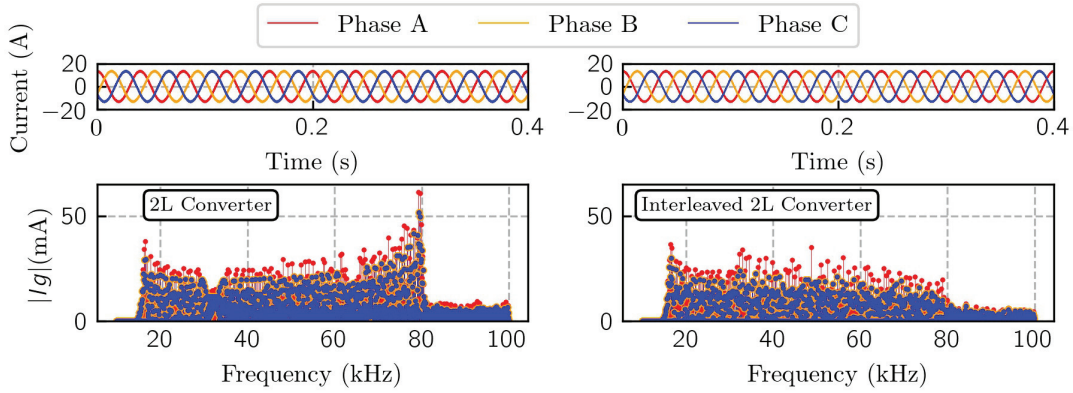

Fig. 8. Overlapping cancellation with interleaved topology.

hard-paralleling) and interleaved (interleaving level=2) 2-level converters with the sinusoidal VSFPWM profile. The system parameters are listed in Table.I. The switching profiles for the non-interleaved and interleaved converters are $f_{\text{c0}} = 48$ kHz, $C_{\text{k}} = 32$ kHz, $\theta_{\text{k}} = 270°$ and $f_{\text{c0}} = 24$ kHz, $C_{\text{k}} = 16$ kHz, $\theta_{\text{k}} = 270°$ respectively to make a fair comparison considering the semiconductor losses. It can be noted from Fig.6 that the grid current harmonic peak near 75 kHz is reduced significantly (about 40%) after the interleaving. This means less filtering requirement for the latter to comply with the same current harmonics emission standard e.g., IEEE519. The measured total-demand-distortion (TDD) from the simulation results are 2.75% and 2.17% respectively, which means, as expected the interleaved converter result in less harmonic injection compared to the non-interleaved one.

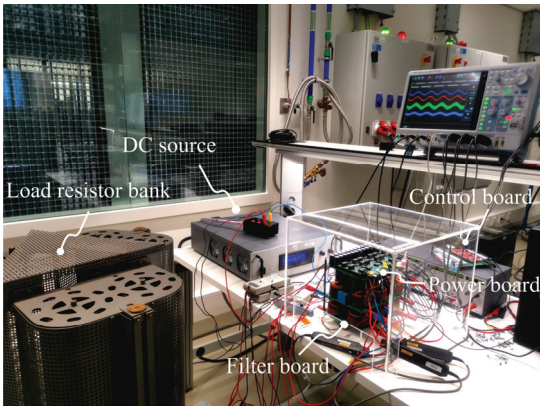

Fig. 9. Experimental set-ups.

V. EXPERIMENTAL VERIFICATION

A 10 kW rated three-phase 2-interleaved 2-level converter, which also works as 2-hard-paralleling converter, is used for the experimental validation of the previous analysis, as shown in Fig.9. The experimental tests have been conducted to verify the symmetry properties as mentioned in Section.III as well as the overlapping cancellation of the harmonic spectra in the interleaving converter. Similar to the simulation, the sinusoidal VSFPWM switching frequency profile is adopted for the experiment. θ_{k} (or in this sinusoidal case θ_1) are selected to be 90° and 270° respectively.

A. Spectra Symmetry between Three Phases

To verify the spectra symmetry between phases, the converter was tested under 2-hard-paralleling topology. Besides the frequency profile: $f_{\text{c0}} = 24$ kHz, $C_{\text{k}} = 2$ kHz, $\theta_{\text{k}} = 0°$ is applied to all three phases. Based on the tested results shown in Fig.10, it can be noted that the spectra of the differential-mode harmonics of the three-phase output voltages under different f_{m} values are very close to the simulated spectra presented in Fig.5(b). The three-phase voltage spectra are not magnitude-symmetrical between phases in the first switching-frequency harmonic band except $f_{\text{m}} = 3f_{\text{o}}$. Therefore, based on both simulation and experimental results it can be concluded that the spectra of both CM+DM and DM components of three phase output voltage are three-phase symmetrical in the first switching-frequency harmonic band when f_{m} equals the triple times of f_{o}. In other cases of f_{m}, the spectra of the three phases are only three-phase balanced but not necessarily three-phase symmetrical. When three different frequency profiles (in same waveform shape but different phase shift) to the three phases, the CM+DM components of the three phases are always three-phase symmetrical.

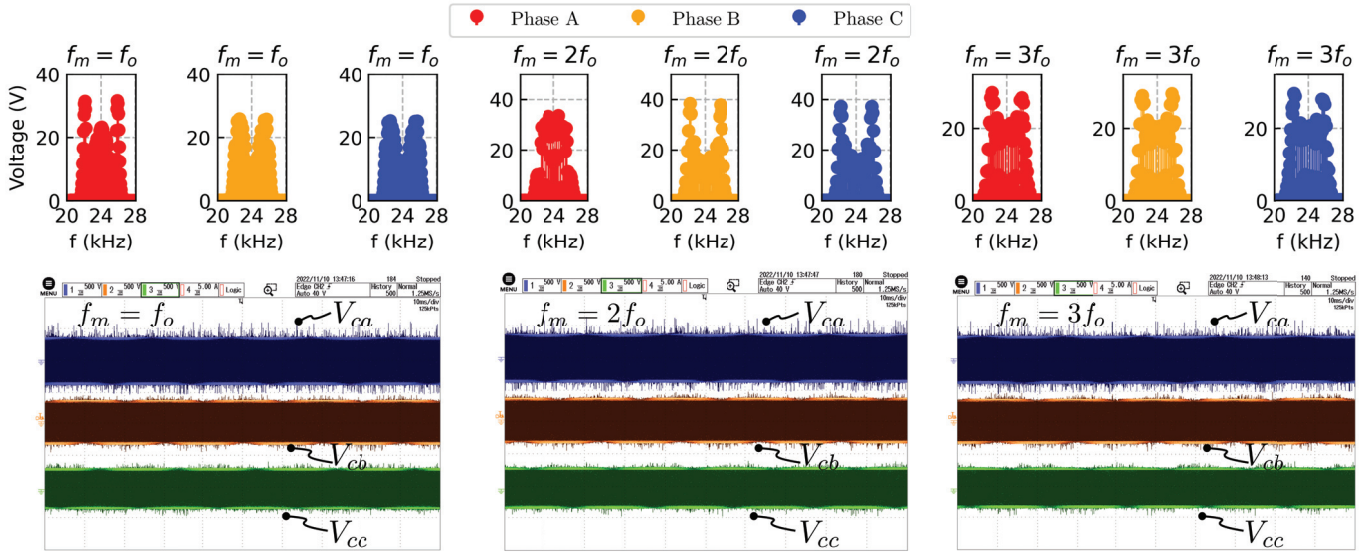

Fig. 10. Experimental waveforms and FFT spectrum of the three-phase converter output voltages (Differential-mode) under different values of f_{m} (same frequency profile for three phases).

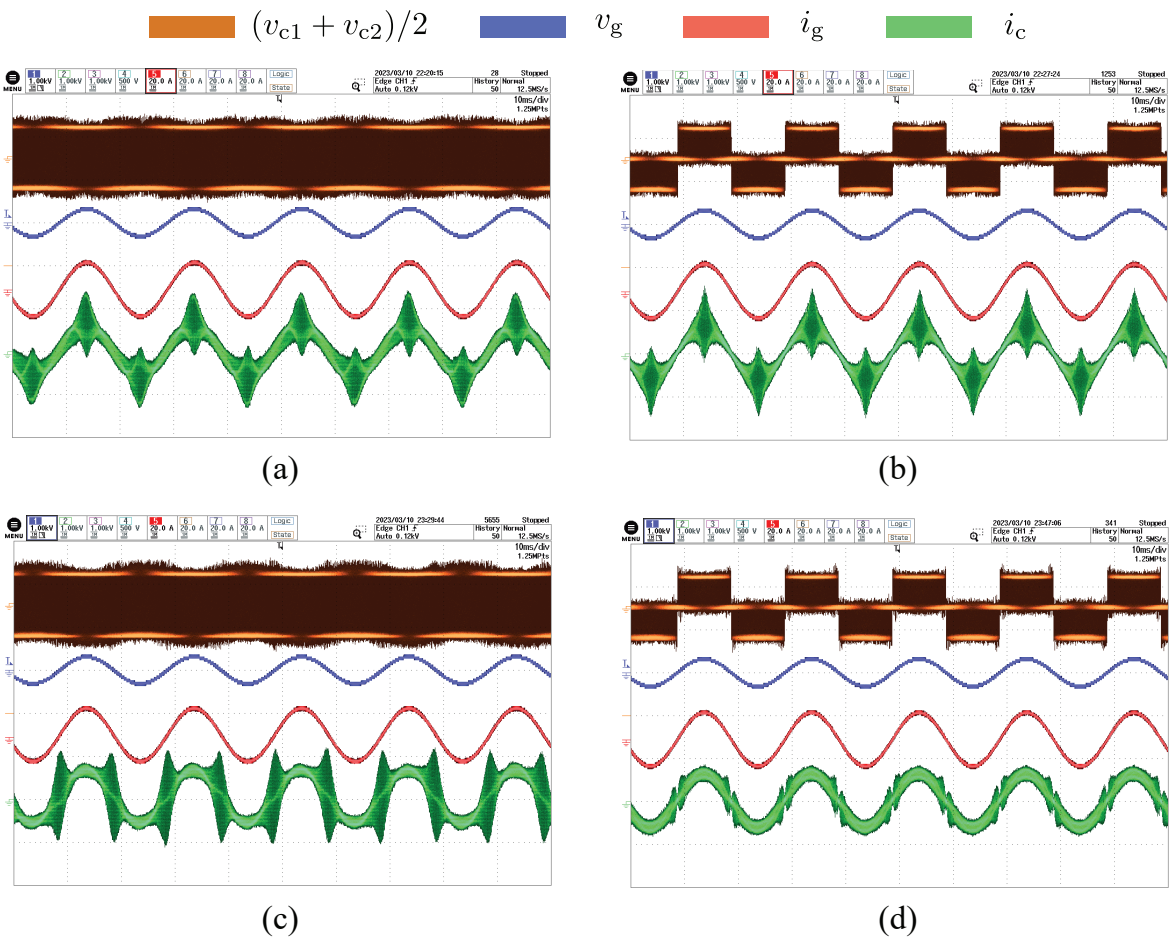

Fig. 11. Experimental waveforms (Phase A) under different test conditions: (a) 2-Hard-Paralleling: $f_{c0} = 48$ kHz, $C_k = 32$ kHz, $\theta_k = 90°$ (b) 2-Interleaving: $f_{c0} = 24$ kHz, $C_k = 16$ kHz, $\theta_k = 90°$ (c) 2-Hard-Paralleling: $f_{c0} = 48$ kHz, $C_k = 32$ kHz, $\theta_k = 270°$ (d) 2-Interleaving: $f_{c0} = 24$ kHz, $C_k = 16$ kHz, $\theta_k = 270°$.

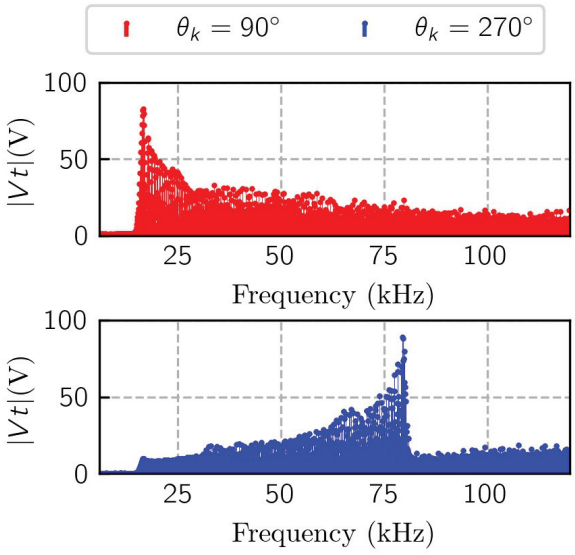

Fig. 12. Experimental harmonic spectrum of output voltage under $f_{c0} = 48$ kHz, $C_k = 32$ kHz with different θ_k (2-hard-paralleling: Phase A).

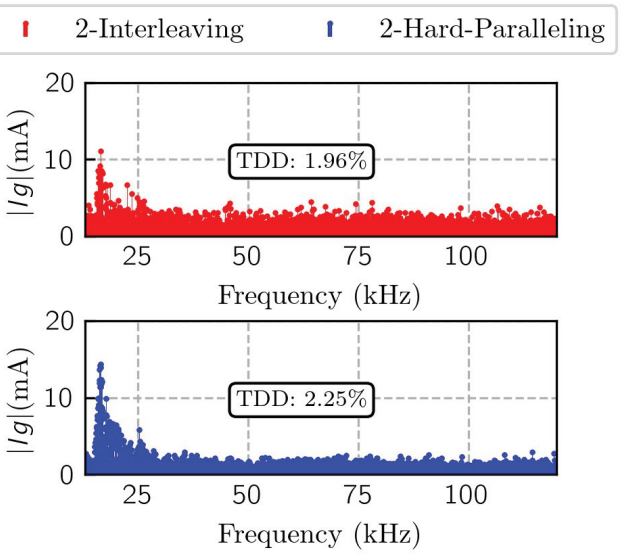

Fig. 13. Experimental grid current harmonic spectrum with 2-Interleaving and 2-Hard-Paralleling (Phase A).

B. Spectrum Symmetry with Different Angle

The tested waveforms of converter output voltage and current as well as the grid-side current from Phase A are shown in Fig.11. Based on the obtained waveforms, the spectra of the 2-hard-paralleling converter output voltage under $\theta_k = 90°$ and $270°$ are depicted in Fig.12 through the Fast-Fourier Transform (FFT) analysis. It can be seen from the harmonics results that the spectrum symmetry depends on θ_k. Additionally, the style of the asymmetry according to θ_k is the same as the simulated results. An insight can be drawn from such an asymmetry style of harmonic spectrum. For P-VSFPWM method, θ_k can be designed to be $270°$ since the asymmetry style of the harmonics reduces the filtering requirement.

C. Overlapping Cancellation with Interleaving

By analyzing the harmonic spectra of the grid-side currents shown in Fig.11, it has been found that the peak current magnitude for 2-interleaving is 11 mA while that for 2-hard-paralleling is 14.4 mA. The peak current harmonic is reduced by 30%, which is close to the simulated results. Besides, the TDD of the grid-side current for 2-interleaving is 1.96% while that for 2-hard-paralleling is 2.25%, which are depicted in Fig.13. Hence, the large peak current harmonic resulted by the harmonic spectra overlapping has been significantly reduced by using interleaving during the implementation of P-VSFPWM method.

VI. Conclusion and Future Work

In this paper, a comprehensive analysis of the harmonic spectrum in the PWM converter caused by periodic VSFPWM (P-VSFPWM) has been conducted, which is useful for the follow-up design of the filter to comply different harmonic emission standards. The symmetry properties under periodic VSFPWM are deeply investigated and some insights are drawn. The overlapping phenomenon due to the large variation band of the VSFPWM profile is presented and avoided by proposing the use of interleaving solution to the PWM converter. Both simulation and experiment results based on the 6.6 kW 2-interleaving/-hard-paralleling PWM converter are exhibited to verify the analysis. In future, the filter design can be combined with the P-VSFPWM design procedures to optimize the supra-harmonics (2-150 kHz) generated by PWM converter.

References

[1] O. Oñederra, I. Kortabarria, I. M. de Alegría, J. Andreu, and J. I. Gárate, "Three-phase vsi optimal switching loss reduction using variable switching frequency," *IEEE Transactions on Power Electronics*, vol. 32, no. 8, pp. 6570–6576, 2017.

[2] D. Jiang and F. Wang, "Variable switching frequency pwm for three-phase converters based on current ripple prediction," *IEEE Transactions on Power Electronics*, vol. 28, no. 11, pp. 4951–4961, 2013.

[3] Q. Li and D. Jiang, "Variable switching frequency pwm strategy of two-level rectifier for dc-link voltage ripple control," *IEEE Transactions on Power Electronics*, vol. 33, no. 8, pp. 7193–7202, 2018.

[4] X. Mao, R. Ayyanar, and H. K. Krishnamurthy, "Optimal variable switching frequency scheme for reducing switching loss in single-phase inverters based on time-domain ripple analysis," *IEEE Transactions on Power Electronics*, vol. 24, no. 4, pp. 991–1001, 2009.

[5] M. Haider, J. A. Anderson, S. Mirić, N. Nain, G. Zulauf, J. W. Kolar, D. Xu, and G. Deboy, "Novel zvs s-tcm modulation of three-phase ac/dc converters," *IEEE Open Journal of Power Electronics*, vol. 1, pp. 529–543, 2020.

[6] J. Chen, D. Sha, J. Zhang, and X. Liao, "An sic mosfet based three-phase zvs inverter employing variable switching frequency space vector pwm control," *IEEE Transactions on Power Electronics*, vol. 34, no. 7, pp. 6320–6331, 2019.

[7] J. Xu, T. B. Soeiro, Y. Wang, F. Gao, H. Tang, and P. Bauer, "A hybrid modulation featuring two-phase clamped discontinuous pwm and zero voltage switching for 99% efficient dc-type ev charger," *IEEE Transactions on Vehicular Technology*, vol. 71, no. 2, pp. 1454–1465, 2022.

[8] J. Balcells, A. Santolaria, A. Orlandi, D. Gonzalez, and J. Gago, "Emi reduction in switched power converters using frequency modulation techniques," *IEEE Transactions on Electromagnetic Compatibility*, vol. 47, no. 3, pp. 569–576, 2005.
[9] Y. Wu, J. Xu, T. B. Soeiro, M. Stecca, and P. Bauer, "Optimal periodic variable switching pwm for harmonic performance enhancement in grid-connected voltage source converters," *IEEE Transactions on Power Electronics*, vol. 37, no. 6, pp. 7247–7262, 2022.
[10] M. Bollen, M. Olofsson, A. Larsson, S. Rönnberg, and M. Lundmark, "Standards for supraharmonics (2 to 150 khz)," *IEEE Electromagnetic Compatibility Magazine*, vol. 3, no. 1, pp. 114–119, 2014.
[11] Z. Qin, L. Wang, and P. Bauer, "Review on power quality issues in ev charging," in *2022 IEEE 20th International Power Electronics and Motion Control Conference (PEMC)*, pp. 360–366, 2022.
[12] L. Wang, Z. Qin, T. Slangen, P. Bauer, and T. van Wijk, "Grid impact of electric vehicle fast charging stations: Trends, standards, issues and mitigation measures - an overview," *IEEE Open Journal of Power Electronics*, vol. 2, pp. 56–74, 2021.